

Survey of ground state neutron Spectroscopic Factors from Li to Cr isotopes

M.B. Tsang^{1*}, H.C. Lee^{1,2}, W.G. Lynch¹

¹*National Superconducting Cyclotron Laboratory and Department of Physics and
Astronomy, Michigan State University, East Lansing, MI 48824*

²*Physics Department, Chinese University of Hong Kong, Shatin, Hong Kong, China*

Abstract

We have extracted the ground state to ground state neutron spectroscopic factors for 79 nuclei ranging in Z from 3 to 24 by analyzing the past measurements of the angular distributions from (d,p) and (p,d) reactions. We demonstrate an approach that provides systematic and consistent values with minimum assumptions. For the 60 nuclei where modern shell model calculations are available, such analysis reproduce, to within 20%, the experimental spectroscopic factors for most nuclei.

* Corresponding author: tsang@nscl.msu.edu

Present and planned rare isotope accelerators offer the opportunities to explore the structure of exotic nuclei, particularly those with large neutron excess. The structure of these nuclei, like their more stable counterparts, reflects interplay between single particle degrees of freedom that govern the shell structure of nuclei [1] and collective degrees of freedom that govern nuclear deformations [2]. The single particle dynamics dictates the shell closure at “magic” neutron or proton numbers, for example. This dynamics can be approximated by the independent particle model, which assumes that nucleons move in a mean field potential [1]. The single particle states of the independent particle model are mixed by the residual nucleon-nucleon interactions [3-5]. Understanding this mixing is an important objective of modern structure calculations, it alters the occupancies or spectroscopic factors of single nucleon orbits from their independent particle model values, and can even modify the “magic” numbers of nuclei at large neutron excess or near the proton drip line [6].

Experimental measurements of the spectroscopic factors for single nucleon orbits within the quantum states of nuclei provide the key experimental probe of single particle dynamics. Both transfer and knockout reactions have been widely studied in order to determine the spectroscopic factors of single nucleon orbits. Transfer reactions comprise the preponderance of such studies in the past four decades, however, their extracted spectroscopic factors often varied widely, reflecting inconsistencies in the choice of optical potentials for the incoming and outgoing channels to which the transfer cross sections are sensitive [7,8]. In this paper, we reanalyze more than 250 neutron transfer reactions and demonstrate that the use of global optical potentials, not available to the earlier studies, allows systematic extraction of spectroscopic factors that are remarkably consistent with large basis shell model calculations [9]. With some modifications, these procedures can be readily extended to rare isotope beam experiments, because it does not require the availability of elastic scattering data for the system being investigated.

In the present work, we focus mainly on the $d+A \Rightarrow p+B$ (d, p) and the inverse $p+B \Rightarrow d+A$, (p, d) reactions and restrict our analysis to ground state to ground state transfers of the neutron from nucleus B to A. These reactions probe the angular momentum, the orbital occupancy and wavefunction of the transferred neutron in the

nuclear surface. The overlap integral between the wave function of one state in nucleus A and another in B defines the theoretical spectroscopic factor for transfer between these states. The ratio of the measured cross-section divided by the calculated cross section using a reaction model provides its experimental counterpart [3-5].

We describe these transfer reactions theoretically as a fast one-step process by calculating the Distorted Born Wave Approximation (DWBA) integral [3-5]. The approach is not strictly the DWBA because we calculate the deuteron optical potential using the Johnson-Soper adiabatic approximation, which corrects for deuteron breakup in the mean field of the target [10]. Following ref. [8], we use the Chapel-Hill 89 [11] global nucleon-nucleus optical potentials and fold those neutron and proton potentials to obtain the deuteron optical potential. We assume nonlocality corrections with range parameters of 0.85 fm and 0.54 fm for the proton and deuteron channels, respectively [12].

We calculate deuteron finite range corrections to the DWBA integral using the local energy approximation (LEA) and the strength ($D_0^2=150006.25 \text{ fm}^3$) and range ($\beta=0.7457 \text{ fm}$) parameters of the Reid soft-core 3S_1 - 3D_1 neutron-proton interaction [13]. For simplicity, we assume a central neutron potential of Woods-Saxon shape with fixed radius ($r_0=1.25 \text{ fm}$) and diffuseness ($a_0=0.65 \text{ fm}$) parameters and adjust the depth of potential to reproduce the experimental binding energy. We use the University of Surrey version of TWOFNR, a direct reaction model code, which provides as options the model assumptions we employ [14]. Other widely used reaction model codes, DWUCK5 [15] and FRESKO [16] yield nearly identical predictions with the same input information [17-19].

Table 1 lists the wide range of nuclei, from ^6Li to ^{55}Cr , studied in this work; it includes transfers with neutron-separation energies ranging from 0.5 to 19 MeV. The extracted spectroscopic factors (SF) and their corresponding uncertainties are listed in the last two columns. The SF values range from very small (<0.1 for ^{20}F , ^{21}Ne , ^{47}Ti) to rather large (~ 7 for ^{48}Ca). In the interest of brevity, details of our evaluation of the data (extracted from more than 250 measurements) will be discussed in another paper [20].

Uncertainties of the present analysis can be estimated by comparing SF value extracted from the pickup (p,d) reaction with those extracted from the inverse stripping (d,p) reaction corresponding to the same ground state neutron transfer. Table II lists the

nuclei used in this comparison; the averaged SF values are listed in the 2nd and 4th columns and the numbers of measurements contributing to these averages are listed in the 3rd and 5th columns. As expected, there is no systematic difference between the spectroscopic factors determined by the (p,d) and (d,p) reactions. As each measurement is independent, the scatter of the data points can be used to assess random uncertainties in the procedure and in the quality of the data. Assuming the fractional random uncertainty of each of the SF values to be the same, we find the data to be consistent with a 20% random uncertainty in each measurement. The same number can be obtained by comparing SF values obtained from the analyses of ground state transfers such as $^{12}\text{C}(\text{d,p})^{13}\text{C}$ [8] and $^{40}\text{Ca}(\text{d,p})^{41}\text{Ca}$ [20] that have been measured over a wide range of d energies. Comparisons of repeated measurements of the same reaction at the same energy suggest that experimental uncertainties may be the dominant contribution to this random uncertainty. Our 20% random uncertainty in (p,d) and (d,p) SF values is less than that deduced by Endt (50%) [21], but they are comparable to the 25% uncertainties that Endt assigned to his “best values” obtained when results from other reactions such as (d,t), ($^3\text{He},\alpha$) are included.

Spectroscopic factors for nuclei with even number of valence neutrons (n) generally exceed those of the neighboring odd n nuclei. This results from the pairing interaction, which couples pairs of neutrons to spin zero similar to the Cooper pairs in a superconductor. For nuclei in the vicinity of a closed shell, this trend can be well replicated by calculations that consider only pairing modifications to the independent particle model [IPM]. Assuming maximal pairing (minimum Seniority), one can obtain a simple relationship between the number of valence nucleons (n) and the spectroscopic factors (S) [3]

$$S = n \quad \text{for } n=\text{even}; \quad S=1-\frac{n-1}{2j+1} \quad \text{for } n=\text{odd} \quad (1)$$

The thin blue bars in Figure 1 shows the predictions of Eq. 1 as a function of the mass number A for the transfer of a $f_{7/2}$ neutron to or from these Ca isotopes; the extracted neutron spectroscopic factors are represented by red stars. The excellent agreement reflects the fact that configuration mixing of $f_{7/2}$ neutrons outside the double magic ^{40}Ca

core is well described by a pairing interaction, with little discernable contribution (at this level) from core polarization or higher lying orbits.

Most nuclei display more significant configuration mixing than these Ca isotopes. The left panel of Figure 2 compares the experimental extracted spectroscopic factors (y axis) and the SF values predicted by Eq. 1 (x axis) for 49 nuclei which have predictions from large basis shell model calculations as explained below. In this figure, we exclude the deformed ^{24}Mg , Li, Ne and F isotopes. This latter group also includes transitions with small calculated or experimental SF values, which, in general, tend not to be as easily calculated or measured. Each element in Fig. 2 is represented by one symbol. Open symbols represent odd Z elements and the closed symbols represent even Z elements. The three different colors of green ($3 \leq Z \leq 8$), blue ($9 \leq Z \leq 18$) and red ($19 \leq Z \leq 22$) represent approximately the p-shell, sd-shell and sdf shell nuclei, respectively. The solid line indicates perfect agreement and the dash line is 50% of the solid line. Most extracted values are less than the IPM plus maximal pairing predictions of Eq. 1. The observed scatter in the data is similar if all available SF values are included in the plot.

A significantly improved description of these nuclei, many of which involve the mixing of several different orbitals, can be obtained by diagonalizing the residual interaction within a large basis shell model [6]. Using Oxbash [22] and the PPN, SPSPDF, SDPN and FPPN interactions [6, 22], the ground state neutron spectroscopic factors for 60 nuclei have been calculated; the uncertainties in the calculations are about 10-20% [6]. The right panel of Figure 2 compares the experimental extracted spectroscopic factors (y axis) and the predicted shell model SF values (x axis). For comparison, the same 49 nuclei are plotted both in the right and left panels. In contrast to the IPM plus pairing calculations, the agreement between data and shell model predictions are within 20% as indicated by the two dashed lines for most cases. For the Ca isotopes, there is close agreement between shell model predictions (thick green bars) and IPM values (thin blue bars) as shown in Figure 1.

Due to the absorption of flux into other channels in the nuclear interior, the DWBA transfer integral samples the neutron bound state wavefunction mainly at the nuclear surface and not in the interior. Transfer constrains the exterior but not the interior contributions to the overlap integral that defines spectroscopic factor. In this analysis, we

assumed a smooth variation of the potential radius ($R=r_0A^{1/3}$) for the bound neutron global potential to avoid the necessity of nucleus by nucleus calculation of bound neutron wavefunction. The good overall agreement between calculated and measured spectroscopic factors indicates that this assumption is reasonable, and that the relative magnitude of transfer spectroscopic factors from nucleus to nucleus appear to be well described. However, the absolute values of the surface contributions to the spectroscopic factor are influenced by these geometrical assumptions.

It has long been asserted that transfer reactions do not yield absolute SF values. Nonetheless, it is informative to compare the results from different reaction mechanisms. The $(e,e'p)$ reaction removes protons from the same orbit for ^{12}C , ^{16}O , and ^{40}Ca isotopes as (p,d) and (d,p) reactions on the transfer reaction removes neutrons. Assuming isospin symmetry, one might therefore expect the spectroscopic factors for (p,d) , (d,p) and $(e,e'p)$ to be comparable for these $N=Z$ nuclei. Because transfer reactions are insensitive to depletions of the orbital occupancy due to hard core interactions in the dense nuclear interior, such effects may cause SF's from $(e,e'p)$, which probes the interior, to be about 10-15% lower than the SF's extracted from transfer. The ground state proton SF values obtained from the $(e,e'p)$ reactions on ^{12}C , ^{16}O , and ^{40}Ca [23] at low momentum transfer, ($Q^2 < 0.2 \text{ GeV}/c^2$) are about 60% of our corresponding ground state neutron spectroscopic factors, however. Interestingly, recent analysis of $(e,e'p)$ data on ^{12}C , ^{16}O at large $Q^2 \geq 1 \text{ GeV}^2$ do not find this large quenching, but report a smaller quenching of the order 10-15% [24, 25] that is consistent with the present results.

Comparisons to knockout reactions with radioactive ion beams can also be made [26,27]. Recent measurements of spectroscopic factors from single-nucleon “knock-out” reactions with radioactive beams and stable nuclei show increasing quenching of the spectroscopic factor values with nucleon separation energy [26, 27]. No such dependence has been reported for $(e,e'p)$ knockout reactions [23]. Within the experimental uncertainties, we also do not see any systematic dependence of quenching of the spectroscopic factors with nucleon separation energy.

Finally, it is interesting to note that the group of light neutron-rich isotopes ^{12}B , ^{16}N , and ^{19}O , with extracted SF values clustering around 0.4 are consistently smaller than the shell model predictions. For such weakly bound nuclei, it is likely that a global

parameterization such as the JLM [28] of the optical model potential in terms of the matter density of the scattering nuclei might be more accurate than the Chappel Hill [11] potential for scattering from such nuclei with diffuse surfaces. The present type of analysis can also be performed using such a potential.

In summary, we have extracted ground state neutron spectroscopic factors from transfer reactions for 79 nuclei using a consistent set of global input parameters and a DWBA integral that includes the effect of deuteron breakup on the (d,p) and (p,d) reactions. We obtain excellent agreement with large basis shell model calculations using an approach that can be readily applied to the new nuclei that will be studied with rare isotope beams. As the nuclear interior is not probed by transfer reactions, absolute spectroscopic factors may not be obtained without additional theoretical input about the interior nucleonic wavefunctions. Nevertheless, we find that transfer reactions to be precise at about the 20% level as a relative measure of the spectroscopic factor over a large range of isotopes. This knowledge is of practical utility when one wants to know neutron spectroscopic factors or to probe nuclei that can only be made in reactions with rare isotopes [19,29].

This work is supported by the National Science Foundation under Grant No. PHY-01-10253 and by the UK Engineering and Physical Sciences Research Council through Grant No. GR/M82141.

References:

- [1] G. Mayer and J. H. D. Jensen, *Elementary Theory of Nuclear Shell Structure* (John Wiley and Sons, London, 1955).
- [2] A. Bohr and B. R. Mottleson, *Nuclear Structure* (Benjamin, New York, 1975), Vol. I
- [3] N. Austern, *Direct Nuclear Reaction Theories*, John Wiley & Sons, New York, 1970.
- [4] G.R. Satchler, *Direct Nuclear Reactions*, Oxford University Press, Oxford, 1983.
- [5] Norman K Glendenning, *Direct Nuclear Reactions*, World Scientific Publishing, 2004.
- [6] B.A. Brown, *Progress in Particle and Nuclear Physics*, 47, 517 (2001).
- [7] C. Iliadis and M. Wiescher, *Phys. Rev. C* 69, 065405 (2004).
- [8] X. D. Liu et. al., *Phys. Rev. C* 69, 064313 (2004).
- [9] B.A. Brown and B.H. Wildenthal, *Ann. Rev. of Nucl. Part. Sci.* 38, 29 (1988).
- [10] R.C. Johnson and P.J.R. Soper, *Phys. Rev. C* 1, 976 (1970).

- [11] R.L. Varner, W.J. Thompson, T.L. McAbee, E.J. Ludwig and T.B. Clegg, Phys. Rep. **201**, 57 (1991).
- [12] F. G. Perey, in *Nuclear spectroscopy and reactions*, edited by J. Cerny (Academic Press, New York, 1974).
- [13] L.D. Knutson, J.A. Thomson and H.O. Meyer, Nucl. Phys. **A 241**, 36 (1975).
- [14] M. Igarashi, M. Toyoma and N. Kishida, Computer Program TWOFNR (Surrey University version).
- [15] P. D. Kunz, DWUCK5, computer program, <http://spot.colorado.edu/~kunz/DWBA.html>
- [16] I.J. Thompson, Comput. Phys. Rep. 7, 167 (1988).
- [17] F. Delaunay et. al., nucl-th/0504045 (2005)
- [18] X.D. Liu, PhD thesis, Michigan State University, (2005).
- [19] N. Keely et. al., Phys. Rev. C **69**, 064604 (2004).
- [20] H.C. Lee et al., to be published.
- [21] P.M. Endt, Atomic Data and Nuclear Data Tables **19**, 23 (1977).
- [22] B. A. Brown et al., Computer program,
<http://www.nsl.msui.edu/~brown/resources/oxbash-augsut-2004.pdf>.
- [23] GJ Kramer, HP Blok and L. Lapikas, Nucl. Phys. A. 679, 267 (2001) and references therein.
- [24] L. Lapikas et al., Phys. Rev. C **61**, 064325 (2000).
- [25] L. Frankfurt, M. Strikman, and M. Zhalov, Phys. Lett. B **503**, 73 (2001).
- [26] A. Gade et. al., Phys. Rev. Lett. **93**, 042501 (2004).
- [27] P.G. Hansen and J.A. Tostevin, Ann. Rev. Nucl. Part. Sci. **53**, 219 (2003).
- [28] J.-P. Jeukenne, A. Lejeune, C. Mahaux, Phys. Rev. C **16**, 80 (1977).
- [29] W.N. Catford, Nucl. Phys. **A 701**, 1c (2002).

Table 1. List of isotopes studied in this work with the extracted spectroscopic factors and other information.

Isotope	shell	SF	err	Isotope	shell	SF	err
⁶ Li	0.68	1.08	0.22	³⁵ S	0.36	0.29	0.06
⁷ Li	0.63	1.82	0.15	³⁷ S		0.88	0.12
⁸ Li	1.09	0.61	0.12	³⁵ Cl	0.32	0.33	0.07
⁹ Be	0.57	0.44	0.03	³⁶ Cl	0.77	0.69	0.14
¹⁰ Be	2.36	1.53	0.15	³⁷ Cl	1.15	1.03	0.15
¹¹ Be	0.74	0.52	0.06	³⁸ Cl		1.74	0.35
¹⁰ B	0.60	0.49	0.07	³⁶ Ar	2.06	3.23	0.46
¹¹ B	1.09	1.34	0.12	³⁷ Ar	0.36	0.35	0.04
¹² B	0.83	0.45	0.06	³⁸ Ar	3.04	2.43	0.49
¹² C	2.85	2.98	0.30	³⁹ Ar		0.79	0.11
¹³ C	0.61	0.79	0.04	⁴⁰ Ar		1.05	0.21
¹⁴ C	1.73	1.56	0.13	⁴¹ Ar		0.55	0.08
¹⁵ C	0.98	1.11	0.22	³⁹ K	1.72	2.10	0.59
¹⁴ N	0.69	0.73	0.08	⁴⁰ K		1.66	0.33
¹⁵ N	1.46	1.38	0.11	⁴¹ K		0.95	0.19
¹⁶ N	0.96	0.42	0.08	⁴² K		0.77	0.11
¹⁶ O	2.00	2.23	0.13	⁴⁰ Ca	4.00	4.30	0.38
¹⁷ O	1.00	0.84	0.04	⁴¹ Ca	1.00	0.99	0.05
¹⁸ O	1.58	1.75	0.20	⁴² Ca	1.81	1.97	0.18
¹⁹ O	0.69	0.41	0.06	⁴³ Ca	0.75	0.62	0.07
¹⁹ F	0.56	1.56	0.22	⁴⁴ Ca	3.64	4.37	0.50
²⁰ F	0.02	0.01	0.00	⁴⁵ Ca	0.50	0.39	0.06
²¹ Ne	0.03	0.03	0.00	⁴⁷ Ca	0.26	0.25	0.04
²² Ne	0.01	0.23	0.03	⁴⁸ Ca	7.38	7.05	0.81
²³ Ne	0.03	0.24	0.03	⁴⁹ Ca	0.92	0.68	0.07
²⁴ Na	0.39	0.56	0.11	⁴⁵ Sc	0.35	0.29	0.06
²⁴ Mg	0.22	0.42	0.08	⁴⁶ Sc	0.37	0.49	0.10
²⁵ Mg	0.34	0.29	0.03	⁴⁶ Ti	2.58	2.38	0.34
²⁶ Mg	2.51	2.79	0.23	⁴⁷ Ti		0.01	0.00
²⁷ Mg	0.46	0.44	0.09	⁴⁸ Ti		0.12	0.01
²⁷ Al	1.10	1.35	0.19	⁴⁹ Ti		0.23	0.03
²⁸ Al	0.60	0.64	0.09	⁵⁰ Ti		6.25	0.63
²⁸ Si	3.62	4.23	0.85	⁵¹ Ti		1.21	0.24
²⁹ Si	0.45	0.37	0.03	⁵¹ V		1.49	0.17
³⁰ Si	0.82	0.72	0.10	⁵⁰ Cr		0.11	0.03
³¹ Si	0.58	0.59	0.07	⁵¹ Cr		0.27	0.04
³² P	0.60	0.53	0.07	⁵² Cr		6.03	0.85
³² S	0.96	1.46	0.41	⁵³ Cr		0.38	0.03
³³ S	0.61	0.67	0.13	⁵⁵ Cr		0.86	0.17
³⁴ S	1.83	1.38	0.20				

Table II: List of nuclei with both spectroscopic factors obtained from (p,d) and (d,p) reactions.

A	A(p,d)B	N _{pd}	B(d,p)A	N _{dp}
¹¹ B	1.25	2	1.44	3
¹¹ Be	0.56	1	0.46	2
¹³ C	0.83	4	0.71	13
¹⁴ C	1.30	4	1.75	2
¹⁵ N	1.41	2	1.33	4
¹⁷ O	0.77	4	0.95	10
¹⁸ O	1.68	2	1.80	1
²¹ Ne	0.03	1	0.03	2
²⁶ Mg	3.07	3	2.51	3
³⁰ Si	0.82	1	0.62	1
⁴² Ca	2.14	2	1.77	3
⁴³ Ca	0.64	1	0.62	2
⁴⁴ Ca	4.16	3	5.00	1
⁴⁸ Ti	0.11	5	0.13	1
⁴⁹ Ti	0.24	2	0.23	1
⁵⁰ Ti	5.14	2	7.36	2
⁵¹ V	1.61	1	1.31	2
⁵³ Cr	0.37	1	0.39	8

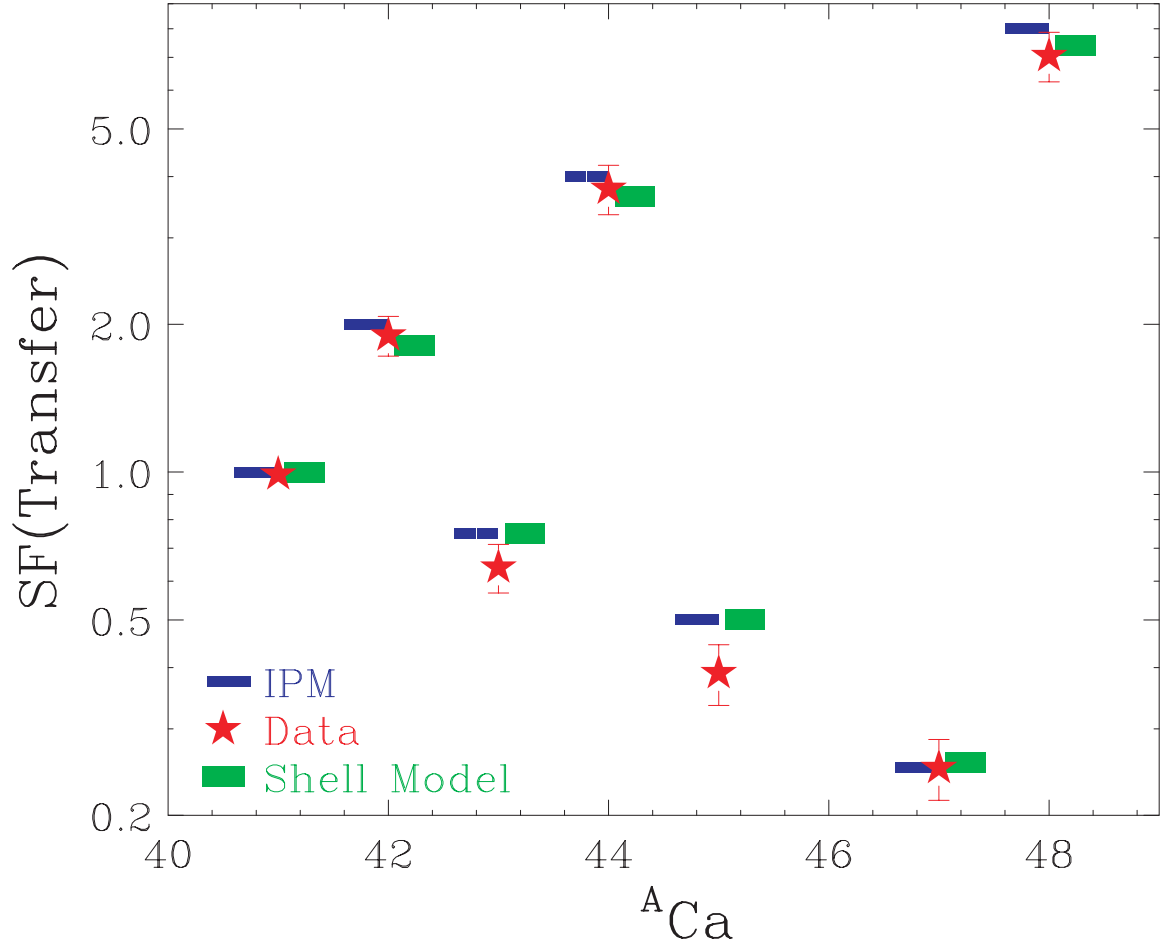


Figure 1 : (Color online) Ground state neutron spectroscopic factors for Calcium isotopes from ^{41}Ca to ^{48}Ca , star symbols represent values extracted from present analysis. Blue lines are IPM values and thick green bars represent predictions from Oxbash. All values are listed in Table I.

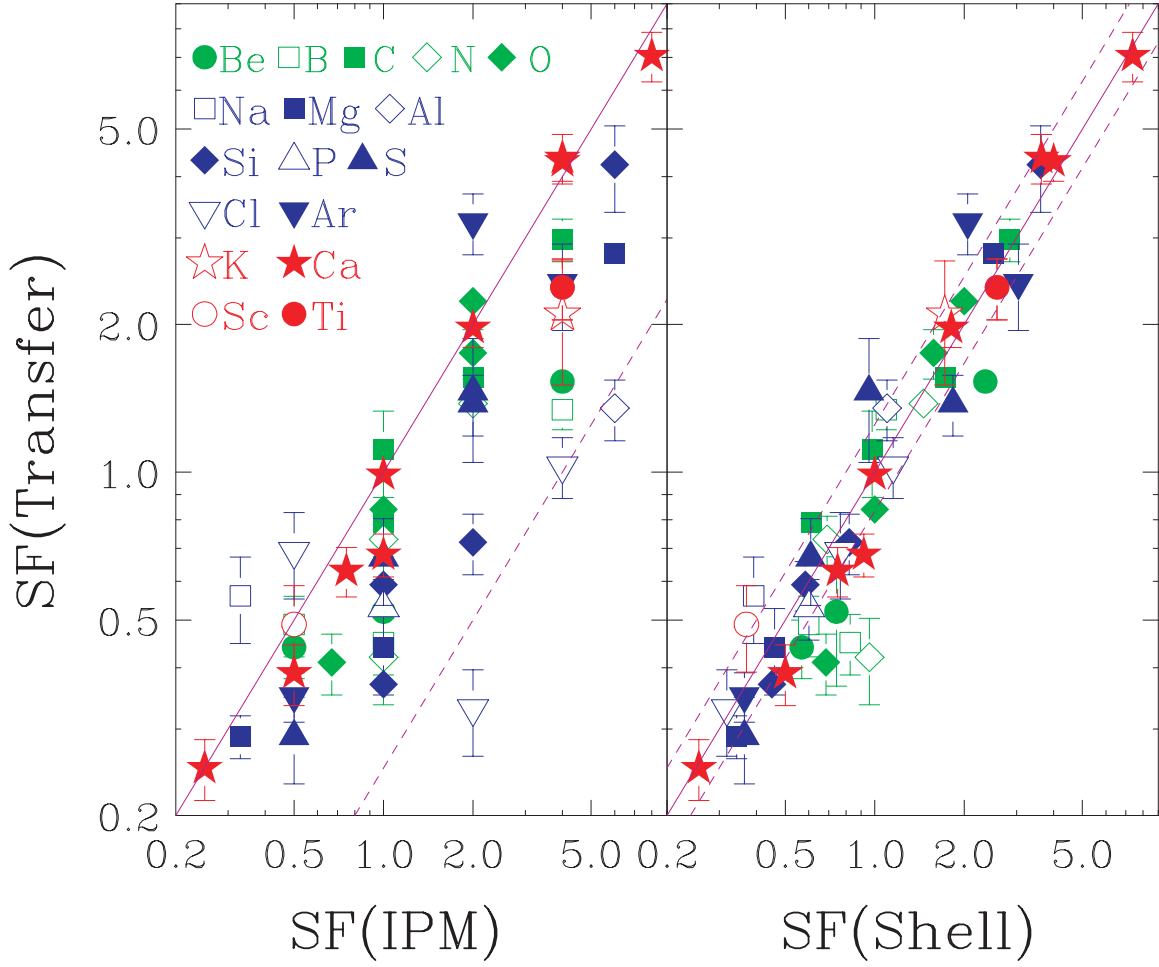


Figure 2 : (Color online) Comparison of experimental spectroscopic factors to predictions from the independent particle model of Eq. (1) (left panel) and shell model program Oxbach (right panel). The solid lines indicate perfect agreement. Dash line in the left panel is 50% lower than the solid line while the two dash lines in the right panel indicate $\pm 20\%$ of the solid line.